

First-Principles Correlated Approach to the Normal State of Strontium Ruthenate

S. Acharya^{1,2,*} M. S. Laad^{3,4,†} Dibyendu Dey¹, T. Maitra⁵, and A. Taraphder^{1,6‡}

¹Department of Physics, Indian Institute of Technology, Kharagpur, Kharagpur 721302, India.

²Department of Physics, King's College London, London WC2R 2LS, United Kingdom

³Institute of Mathematical Sciences, Taramani, Chennai 600113, India

⁴Max-Planck Inst. fuer Physik Komplexer Systeme,

38 Noethnitzer Strasse, 01187 Dresden, Germany

⁵Department of Physics, Indian Institute of Technology, Roorkee, Roorkee 247667, India and

⁶Centre for Theoretical Studies, Indian Institute of Technology Kharagpur, Kharagpur 721302, India.

The interplay between multiple bands, sizable multi-band electronic correlations and strong spin-orbit coupling may conspire in selecting a rather unusual unconventional pairing symmetry in layered Sr_2RuO_4 . This mandates a detailed revisit of the normal state and, in particular, the T -dependent incoherence-coherence crossover. Using a modern first-principles correlated view, we study this issue in the actual structure of Sr_2RuO_4 and present a unified and quantitative description of a range of unusual physical responses in the normal state. Armed with these, we propose that a new and important element, that of dominant multi-orbital charge fluctuations in a Hund's metal, may be a primary pair glue for unconventional superconductivity. Thereby we establish a connection between the normal state responses and superconductivity in this system.

INTRODUCTION

Unconventional superconductivity (USC) in layered Sr_2RuO_4 has long attracted intense attention¹ owing to the expectation that it is a superconducting analogue of superfluid ^3He , with a spin-triplet, odd-parity and chiral order parameter, described by $\Delta(\mathbf{k}) \simeq (k_x + ik_y)\mathbf{z}^2$. Such a state would support half-quantum vortices and topologically protected chiral Majorana modes at the sample edges or on domain walls, which would be of fundamental interest. However, a surge of recent data points toward a much more interesting picture. A range of data also attests to the presence of line nodes in the SC gap function³. Moreover, presence of sizable spin-orbit coupling (SOC) and multi-orbital character of the system dictate that the multi-band pair function reflect spin-orbital entanglement; *i.e.*, it cannot be classified as spin singlet or triplet¹. It is fair to say that determination of the actual pair symmetry in Sr_2RuO_4 continues to be a fascinating open issue. Since the USC is an instability of the highly correlated Fermi liquid (FL) state in Sr_2RuO_4 , resolution of this puzzle mandates a proper microscopic description of the normal state itself. Over the years, extensive experimental studies reveal (*i*) a T -dependent incoherence-coherence (IC-C) crossover from an incoherent high- T metal to a strongly correlated FL metal. The latter obtains only below $T_{FL} \simeq 20 - 25$ K, while signatures of an unusual metallic state¹ are evidenced in a range of transport and magnetic fluctuation data for $T > T_{FL}$. (*ii*) A careful de-Haas van-Alphen (dHvA)⁴ study has mapped out the low- T ($< T_{FL}$) multi-sheeted Fermi surface (FS). Very recent correlated first-principles calculations⁵⁻⁷ show that it is necessary to adequately include the complex interplay between one-electron band structure, local multi-band interactions and SOC to get a quantitative accord with dHvA data. Moreover, the IC-C crossover has been interpreted in terms of Hund's metal physics⁸⁻¹⁰, where sizable influence of Hund cou-

pling (J_H) drastically reduces the lattice-FL crossover scale. However, there is still no consensus on the details of the normal state (spin and charge) fluctuation spectra that can generate the specific pair interaction needed to describe the SC pair symmetry constrained by multitude of data.

MODEL AND FORMALISM

Motivated thereby, we undertake a correlated first-principles theoretical approach using a combination of density functional theory and dynamic mean-field theory (DFT+DMFT) to address these issues. As an impurity solver, we use continuous-time quantum Monte Carlo (CTQMC)¹¹, extended to low T to access the IC-C crossover. Armed with excellent accord with the Fermi surface data, we present a detailed quantitative account of the IC-C crossover, and arrive at a very good quantitative accord with a wide range of normal state responses. We find, for the first time, that a surprising element, namely, nearly singular inter-orbital charge fluctuations involving the $\text{Ru} - 4d$ xy, yz, zx bands, arise due to the complex interplay between orbital-selectivity and SOC. We discuss the implications of this surprising finding for various proposals for USC that emerges in Sr_2RuO_4 from the correlated FL at low T .

Band structure calculations were performed in the real body-centered tetragonal (BCT-space group Immm/139) structure. We first perform ab-initio density functional theory calculations within GGA and GGA+SO for Sr_2RuO_4 using the full potential linearized augmented plane-wave (FP-LAPW) method as implemented in the WIEN2k code¹². We perform Wannierization of the Wien2k output bands around the Fermi level via interface programs like WANNIER90¹³, WIEN2WANNIER¹⁴. This would, in turn, give us the Wannier orbitals around the Fermi level which serve as inputs of the DMFT

self-consistency calculation. Three t_{2g} bands, comprising a two-dimensional xy -like γ band and a quasi-one-dimensional β (xz - yz -like) band, both electronlike, and a quasi-1D holelike α -band (xz - yz -like) cross E_F . In line with several data that point to sizable SOC, the FS topology is correctly reproduced in DFT only when SOC is included. However, sizable multi-band electronic correlations are mandatory to obtain quantitative accord with the dHvA FS⁷. The interplay between multiband correlations and SOC will also be crucial to quantitatively describe the IC-C crossover. Thus, use of a realistic Hubbard model for the t_{2g} bands with real structural input and SOC is mandatory. The model we use⁷ is the three-band Hubbard model:

$$H = H_{DFT} + H_{loc} - H_{dc} \quad (1)$$

where $H_{DFT} = \sum_{\langle i,j \rangle} \sum_{\sigma,\sigma'} \sum_{a,b} t_{a\sigma,b\sigma'}^{ij} c_{ia\sigma}^\dagger c_{jb\sigma'}$, $c_{ia\sigma}^\dagger$ creates an electron in a Wannier state in orbital a with spin- σ , etc, H_{dc} is the double-counting correction, and the $t_{a\sigma,b\sigma'}^{ij}$ are the hopping integrals including the SOC term⁷. H_{loc} describes the direct, exchange, pair-hopping and spin-flip terms in the onsite t_{2g} basis.

The interaction matrix is

$$\begin{pmatrix} 0 & U & U - 3J & U - 2J & U - 3J & U - 2J \\ U & 0 & U - 2J & U - 3J & U - 2J & U - 3J \\ U - 3J & U - 2J & 0 & U & U - 3J & U - 2J \\ U - 2J & U - 3J & U & 0 & U - 2J & U - 3J \\ U - 3J & U - 2J & U - 3J & U - 2J & 0 & U \\ U - 2J & U - 3J & U - 2J & U - 3J & U & 0 \end{pmatrix}$$

in the basis $xy \uparrow, xy \downarrow, xz \uparrow, xz \downarrow, yz \uparrow, yz \downarrow$. In the D_{4h} site symmetry, the t_{2g} states split into a b_{2g} singlet (xy) and e_g doublet (xz, yz), with $\epsilon_{xz} - \epsilon_{xy} = E_{cf} \simeq 120$ meV being the crystal field splitting. In view of this observation, we work with bare values of $U_{ll',mm'}$ with $l, l', m, m' = a, b$ taken to be orbital-independent, with the understanding that these will effectively acquire orbital dependence due to crystal field effect above.

RESULTS

We begin by discussing our first-principles correlated approach including SOC, which gives the actual correlated Fermi surface for Sr_2RuO_4 . The bare SOC ($\simeq 90 - 130$ meV) is roughly of the order of the crystal field splitting at the DFT level. Inclusion of sizable d -shell correlations has many effects:

(i) Correlation effects are larger for the xy -orbital states, since they lie lower in energy and are more populated. On the other hand, the smaller band widths of the $d_{xz,yz}$ orbital states mean a larger effective U/W (W =bandwidth) ratio for these. This introduces an effective orbital-dependent Hubbard U for the three t_{2g} orbital states, with $U_{xy,xy} > U_{xz(yz),xz(yz)}$, mimicking the situation derived recently by Pavarini *et al.* This causes an

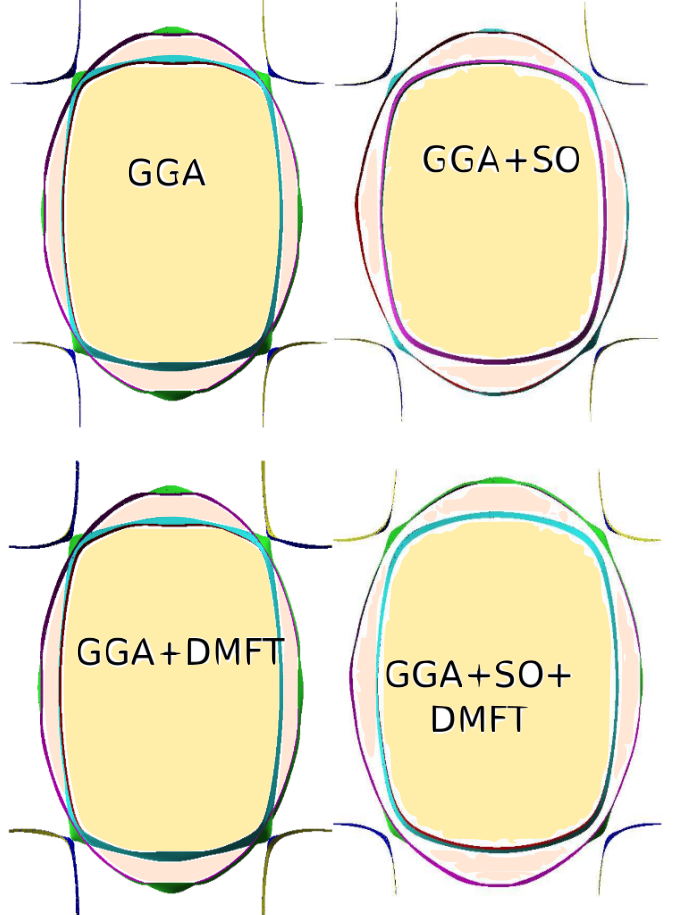


FIG. 1. Fermi surfaces for Sr_2RuO_4 calculated using GGA, GGA+SO, GGA+DMFT, GGA+SO+DMFT. In agreement with Pavarini *et al.*, We find that SOC is essential to derive the quantitatively correct Fermi sheets as seen in dHvA experiment of Bergemann *et al.*

effective anisotropy in the d -shell Coulomb interactions and is indeed the basic mechanism that sets the stage for orbital-selectivity to emerge.

(ii) Due to inter-orbital charge transfer caused by the interaction terms associated with $\sum_{i,\sigma,\sigma'} n_{i,xy,\sigma} n_{i,xz(yz),\sigma'}$, the bare crystal field splitting is renormalized already at the Hartree level, to an effective value less than its bare DFT value. Since the SOC coupling constant is weakly enhanced by correlations (a simple way to see this is that the static Hartree-Fock contribution from the Hund term directly renormalizes the bare SOC, so $\lambda_{soc}^{eff} = \lambda_{bare} + J \langle c_{ia\sigma}^\dagger c_{ib\sigma'} \rangle$), the ratio of the effective SOC to the effective crystal field splitting is enhanced upon switching on electronic correlations. This means that it is no longer possible to disentangle orbital and spin degrees of freedom, a feature which must have far-reaching consequences for the detailed symmetry of the pair wavefunction in Sr_2RuO_4 .

Both these effects directly bear upon the renormalized electronic structure and the Fermi surface topology. In

Fig. 1, we exhibit the GGA, GGA+DMFT, GGA+SOC and GGA+SOC+DMFT Fermi surfaces. It is clear that GGA+DMFT alone gives Fermi surfaces in discord with dHvA data, and that inclusion of SOC is mandatory to obtain correct Fermi surface sheets with regard to their shapes and size⁷.

In addition, these changes in the bare DFT parameters cause changes in dynamical spectral weight transfer, caused by higher order terms in the self-energy in DMFT. Thus, effective mass enhancements will be orbital-dependent in the low- T FL state, as is known⁴, and different bands are narrowed down to differing extent. The average effective mass enhancement at 30 K is $O(3 - 4)$, in excellent accord with both dHvA estimates and specific heat data. The coherent part of the “renormalized band structure” could be tested against ARPES band structures in future. More importantly, we find that the orbital character of the three t_{2g} bands is sizably \mathbf{k} -dependent due to momentum-dependent spin-orbital entanglement. This is a crucial input when one considers the construction of a “pair interaction” to obtain USC: the pair interaction must also reflect this spin-orbital entanglement. We leave this aspect for future studies.

Armed with this accord, we now study the normal state responses in Sr_2RuO_4 in detail. In Fig 2, we show the full one-electron local Green function in imaginary time, $G(\tau)$ as a function of $T(> T_{FL})$. Very good collapse of all curves on to a single curve is clear and, upon careful fitting with a “local” quantum-critical form, $G(\tau)/G(\beta/2) \simeq c_0 \sin(\pi\tau/\beta)^{-(1-\alpha_g)}$ with $\alpha_g = 0.32$. This conformal-invariant form is that expected for a locally quantum-critical metal, where the infra-red pole structure of $G(\omega)$ in a FL metal is supplanted by an infra-red branch-cut continuum form with anomalous fractional exponents. Correspondingly, Fig 2 shows that the self-energies also exhibit anomalous behavior: $\text{Im}\Sigma(i\omega) \simeq (i\omega)^{1-\eta(T)}$ up to rather high energies. Remarkably, the dynamical spin susceptibility also exhibits similar scaling behavior: in Fig. 2, clear collapse of $\chi_s(\tau)$ to a universal scaling function, given by $\chi_s(\tau)/\chi_s(\beta/2) \simeq c_1 \sin(\pi\tau/\beta)^{-(1-\alpha_s)}$, with $\alpha_s \simeq 0.93$ is seen. This is precisely the form expected for an intermediate $T(> T_{FL})$ state exhibiting conformal invariance. Using a well-known trick, the real-frequency local dynamical spin susceptibility is then obtained as $\text{Im}\chi_s(\omega, T) \simeq c_1 T^{\alpha_s} F(\omega/T)$, where $F(y)$ is a universal scaling function of y^{15} .

Microscopically, a reason for these findings is that the Hubbard $U = 2.3$ eV is larger than the band-width of xz, yz bands ($W_{xz,yz} = 1.4$ eV), while it is comparable to that of the xy -band. Thus, depending upon the orbital, one is effectively either in the intermediate (xy) or the strong-coupling (xz, yz) of the three-band Hubbard model, with non-integer occupation of each orbital. In the xz, yz -sector, we now expect a tendency to have orbital-selective Mott-like states. At high T , the inter-orbital hybridization is effectively rendered irrelevant by sizable J_H (Hund’s metal scenario), and thus

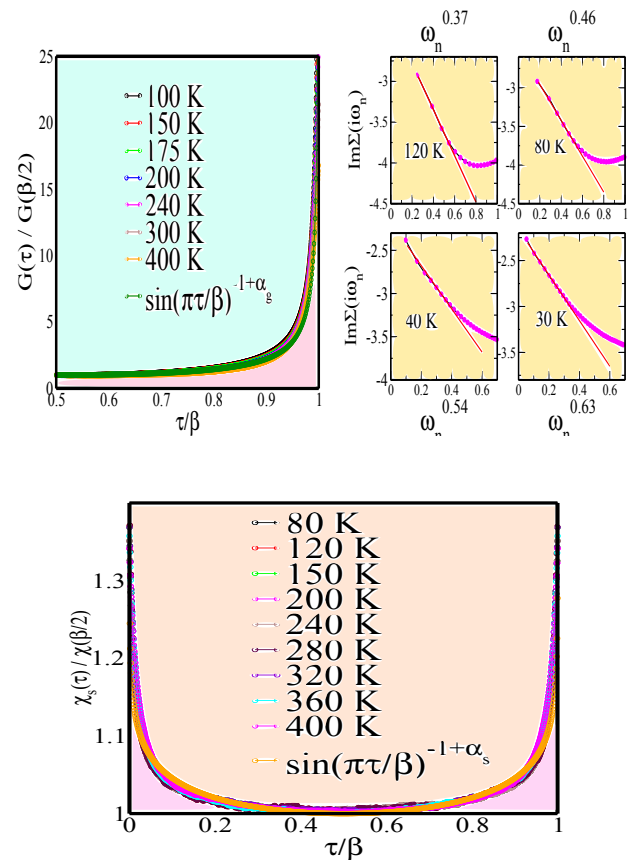


FIG. 2. Imaginary parts of the scaled one-electron Green function (top left) and the scaled dynamical spin susceptibility (bottom) as functions of τ/β . For $T > T_{FL} \simeq 30$ K, both exhibit clear local quantum-critical scaling behavior with different exponents (see text), implying strange metallicity in Sr_2RuO_4 above 30 K. The imaginary parts of the self-energy (top right) as a function of $i\omega_n$: clear anomalous power-law behavior up to high energy $O(0.5)$ eV further testifies to anomalous metallicity for $T > 30$ K.

one deals with an effective situation where there is strong scattering between metallic (xy) and effectively localized (xz, yz) carriers. In the local impurity model of DMFT, this implies that the latter cannot recoil during an interband scattering process, leading to emergence of recoil-less X-ray edge physics. The high- T infra-red singularities in one- and two-particle propagators we find in DMFT are thus associated with local processes akin to those occurring in the seminal orthogonality catastrophe¹⁶.

Remarkably, these results offer direct insight into the high- T anomalies characteristic of Sr_2RuO_4 . First, transport can now be rationalized solely in terms of the structure of $G_{loc}(\omega)$ or $\Sigma_{loc}(\omega)$, since local irreducible vertex corrections are negligible¹⁷ in multi-orbital DFT+DMFT. Explicitly, using results above, we find

that the *dc* resistivity, $\rho_{dc}(T) \simeq T^{2(1-\alpha_g)} \simeq T^{1.0} - T^{1.5}$, which is qualitatively consistent with observations above $T_{FL} \simeq 30$ K¹ right up to 900 K. Correspondingly, the optical conductivity, $\sigma(\omega) \simeq \omega^{-2(1-\alpha_g)} \simeq \omega^{-1.0}, \omega^{-1.3}$. This also implies anomalous energy-dependent scattering rate, $\tau^{-1}(\omega) \simeq \omega^{1.0}, \omega^{1.3}$, and energy-dependent effective mass enhancement, $m^*(\omega)/m_b \simeq \omega^{-1.0}, \omega^{-1.3}$. Remarkably, both these features seem to be in accord with data (see Fig.(4) of Katsufuji *et al.*¹⁸, and our results suggest a re-interpretation of the $T > T_{FL}$ transport data within an incoherent metal scenario (indeed, no FL contribution is seen down to 0.03 eV in optical data for $T > T_{FL}$). Moreover, the local critical form of the dynamical spin susceptibility permits rationalization of the anomalous neutron and NMR results above T_{FL} as follows: $y = \omega/T$ -scaling in $\chi_s(\omega, T)$ with an exponent $(1 - \alpha_s) \simeq 0.93$ implies that $\omega^{0.933} \text{Im}\chi_s(\omega, T)$ must be a universal scaling function of y for $T > T_{FL}$. This is fully borne out by neutron scattering data above 30 K¹⁹, which is precisely the crossover scale for FL behavior. In addition, $\alpha_s = 0.933$ is also close to the exponent of 1.0 used to fit the neutron scattering intensity for $\omega > 2.0$ meV^{20,21}. Finally, the full-width at half-maximum, related to the damping of magnetic excitations must scale as $(\omega, T)^{1-\alpha_s} \simeq (\omega, T)^{0.933}$, again in excellent accord with data. The NMR spin relaxation rate should vary as $1/T_1 = T \lim_{\omega \rightarrow 0} \frac{\text{Im}\chi_s(\omega, T)}{\omega} \simeq T^{-0.93}$, implying a sizably T -dependent (but increasing with reduction of T) $1/T_1$ for $T > T_{FL}$: this is also not inconsistent with data²² for $\mathbf{H} \parallel c$. Thus, good accord with a range of normal state responses lends strong support to an intermediate- T local non-FL “strange” metallic state in Sr_2RuO_4 .

In contrast to high- T_c cuprates however, Sr_2RuO_4 shows a smooth crossover from the high- T non-FL metal to a correlated FL metal below $T \simeq 30$ K. Understanding the nature of this crossover is mandatory to uncover the microscopics of USC setting in below $T_c = 1.5$ K. We have done a careful extension of CTQMC to reach $T \simeq O(12)$ K, allowing us to study this IC-C crossover in detail. In Fig. 2, we exhibit evidence for gradual restoration of FL-like metallicity at low T , which is signalled by the fact that the $\omega = 0$ intercept in $\text{Im}\Sigma(i\omega)$ approaches zero as T is lowered.

This is also borne out by the observation that the orbital-dependent effective masses acquire sizable enhancement (SI2), become almost T -independent, along with drastically reduced scattering rate below $T \simeq 23$ K, in excellent accord with indications for a low- T correlated FL metal from optical data¹⁸. In fact, the effective masses for all orbitals are enhanced by a factor of about 3 – 4 at low T , in nice accord with specific heat data²¹. Since the out-of-plane resistivity also acquires a T^2 dependence below T_{FL} , this evidences that a dimensional crossover is implicated in the non-FL-to-FL crossover. In a quasi-2D correlated FL, this crossover should occur when $k_B T \simeq t_{\perp}$, the one-electron hopping between weakly coupled layers. One might then wonder whether

(and how) the strong incoherent metal signatures found for $T > T_{FL}$ influence this crossover. We now provide a detailed analysis of this aspect, showing how “high- T ” incoherence indeed dramatically affects details of the low T FL state in ways incompatible with a simple one-electron band-structural view.

Physically, at low T , the interband hybridization eventually gets relevant at a scale pushed dramatically downward by Hund metallicity, introducing recoil into the local impurity model, and cutting off the infra-red singularities found for $T > T_{FL}$. To consider this crossover as a function of T , we observe that: (i) the interlayer hopping, $t_{\perp} \simeq 0.02\text{eV}(200\text{K}) \parallel t_{a\sigma, b\sigma}^{-1}$, even in the renormalized DMFT electronic band structure, and (ii) at high T , the c -axis resistivity shows insulator-like behavior in contrast to the bad-metallic in-plane resistivity. These arguments show that a dimensional crossover from effectively decoupled 2D layers (at high T) to an anisotropic 3D state is implicated in the IC-C crossover. A description of the effect of t_{\perp} requires consideration of a model with coupled RuO_2 layers. Since the interlayer hopping for the d_{xy} band is much smaller than for the $d_{yz, zx}$ bands in the undistorted BCT structure, we are led to consider the effective model of two coupled quasi-1D xz, yz bands to facilitate the description of the IC-C crossover as a dimensional crossover, driven by increasing relevance of coherent one-electron inter-orbital mixing at lower T :

$$H = \sum_{i, a \neq b = xy, yz, zx} H_{1D}^a - \sum_{i, a, b, \sigma} t_{\perp} (C_{ia\sigma}^{\dagger} C_{ib\sigma} + h.c) \quad (2)$$

where $\nu, \nu' = xz, yz$. We now discuss the IC-C crossover and the associated dimensional crossover with a somewhat subtle analytic framework. For a system of coupled 1D-like chains as above, a description of this crossover by perturbation theory in t_{\perp} in the non-FL metal is beset with difficulties, and is valid only in the non-FL regime, but fails to reproduce the FL regime. Perturbation approaches in interaction, beginning from the free band structure work in the FL regime, but fail in the non-FL regime. An attractive way out is provided by a close generalization of a non-trivial argument developed in the context of coupled Luttinger chains¹⁷. In our case, each RuO_2 layer is connected via t_{\perp} to z_{\perp} nearest neighbors, with $z_{\perp} \rightarrow \infty$.

Rigorously, one needs a numerical solution for the full local propagator, $G(k, \omega)$, which we take from our DFT+DMFT calculation. Using this input, we can draw qualitative conclusions regarding the effect of non-FL metallicity at high- T on the non-FL to FL crossover at lower T as follows. In the non-FL regime, for each of the quasi-1D xz, yz bands, the in-plane self-energy $\Sigma_{\nu}(\omega) \simeq (t(\omega)/t)^{1/(1-\alpha)}$ ¹⁷. It is clear that t_{\perp} becomes relevant, inducing the dimensional crossover when $t_{\perp}^{a,b} > \Sigma_a$, yielding the crossover scale $E^* \simeq t_{\perp}(t_{\perp}/t)^{\alpha/(1-\alpha)}$. With $\alpha = 0.32$ in our case, this yields $E^* \simeq 40$ K, in good accord with the numerical estimate of 23 K in numerics .

Once $T < E^*$, one ends up with an anisotropic correlated FL metal. In particular, when $t_\perp \ll t$ and at low energies, all one-particle quantities obey the scaling $\omega' = \omega/E^*$, and $T' = T/E^*$; i.e., $t\Sigma(\omega, T) = E^* t_\perp \Sigma'(\omega', T')$ and $tG(\omega, T) = (E^*/t_\perp)G'(\omega', T')$ where Σ and G are universal functions associated with the crossover. A low-frequency expansion of Σ in the FL regime gives the quasiparticle residue $Z \simeq (t_\perp/t)^{\alpha/(1-\alpha)} = E^*/t_\perp$. The inter-layer resistivity, $\rho_\perp(T)/\rho_0 = (t/E^*)R(T/E^*)$ with $R(x \ll 1) \propto x^2$ and $R(x \gg 1) \propto x^{1-2\alpha}$. And the resistivity enhancement, $\rho_\perp(T)/\rho_0 = A(T/t)^2$ with $A = (t/t_\perp)^{3/(1-\alpha)}$. The resulting anisotropy of the Woods-Saxon ratio, $A_c/A_{ab} = (a/c)^2 A \simeq 1000$ for $\alpha = 0.32$, which is indeed in the right range¹. Finally, the c -axis optical response is incoherent above E^* , with a coherent feature carrying a relative weight $\simeq Z^2$ appearing at low- T , again in qualitative agreement with observations¹⁸. An obvious inference from the above is that increasing T should lead to a disappearance of the quasicoherent features in photoemission. This may already have been observed experimentally²³.

The above arguments show how high T incoherence stemming from effectively 1D xz, yz states drastically affects details of the IC-C crossover. At low- T , in the correlated FL regime, DMFT(CTQMC) provides a consistent description of electronic correlations and lead to very good quantitative accord with dHvA and mass enhancements, as shown above. In our picture, therefore, the effective mass enhancement arises from renormalization effects caused by local multiband electronic correlations (DMFT). This completes our qualitative description of the non-FL to FL crossover, where the “high”- T non-FL metal is taken to be the local critical metal. Thus, the physical mechanism for this crossover (which is also a dimensional crossover) is the increasing relevance of the inter-layer one-electron hopping at lower T , since the SOC seems to become relevant at lower T as reflected in the in-plane versus out-of-plane spin susceptibility anisotropy¹.

To further characterize this crossover and search for a dominant electronic pair “glue”, we computed the T -dependent local spin ($\chi_s(T)$) and orbital-resolved charge ($\chi_{a,ch}(T)$, with $a = xy, yz, xz$) susceptibilities. In Fig. 3, we show $\chi_s(T)$ from high- up to low T . Clear Curie-Weiss like behavior at high T smoothly crossing over to a high but relatively T -independent value at low $T < 23$ K is a manifestation of the non-FL-to-FL crossover. Moreover, we find a high-spin state ($S = 1$) on Ru, and thus a Hund metal, arising from sizable Hund coupling. Several points are in order: (i) details of the T -dependence of $\chi_s(T)$ are in good accord with data if one assumes²⁰ a “relaxor” form $\chi_s(q, \omega) = f(q)\chi_s^{loc}(\omega)$ with $\chi_s^{loc}(\omega, T)$ evaluated within DMFT as above. Due to enhancements at incommensurate \mathbf{q}_{in} coming from the quasi-1D xz, yz bands (which enter via the factor $f(q)$ in an RPA like view), the relevant quantity to compare is $\chi_s(\mathbf{q}_{in}, \omega, T)$. Assuming, in spirit of DMFT, that the T -dependence is dominantly in χ_s^{loc} , we find surprisingly

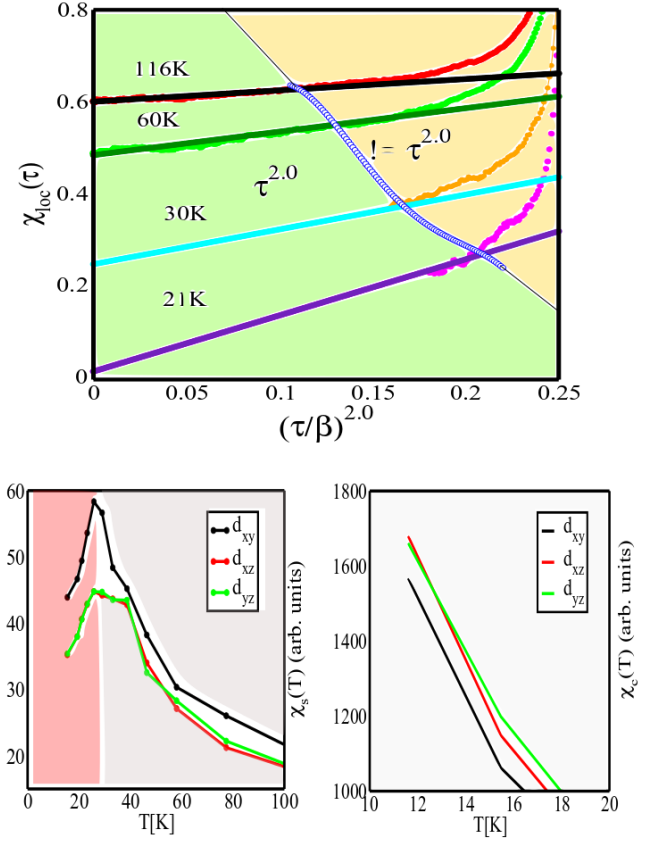


FIG. 3. Gradual restoration of correlated Landau Fermi liquid as T is lowered below 30 K, as seen by the fact that the intercept on the $\chi_{loc}(\tau)$ axis vanishes at $\simeq 21$ K (top). The $\chi_{loc}(\tau)$ is τ^2 (Fermi Liquid like) for finite low energies and finally deviate from τ^2 across the blue boundary where incoherence sets in. With lower temperatures the FL liquid behavior sustains over larger energy ranges, showing predominance of coherence. The incoherence-coherence crossover is reflected in the change in the T -dependent band-resolved spin susceptibilities around 30 K (bottom left). We show that the orbital-resolved charge susceptibilities are enhanced relative to the spin susceptibility at low T , making them attractive candidates for an electronic pair glue (bottom right).

good accord with data over the whole T range, right down to 23 K, where $\chi_s(q_{in}, T)$ flattens out. However, the orbital-resolved charge susceptibilities spring a surprise: in Fig. 3, we show that $\chi_{a, ch}(T)$ for $a = xz, yz$ is enhanced relative to $\chi_{xy, ch}(T)$, and, more importantly, that $\chi_{a, ch}(T)$ always increases at lower T without flattening out, at least down to 12 K. We expect $\chi_{a, ch}$ to eventually approach an enhanced T -independent value at low T (since the metallic state immediately above $T_c = 1.5$ K is a FL), but we are unable to access this possibility numerically below 12 K. It is also noteworthy that $\chi_{xy, ch}$ is comparably enhanced at low T . Our finding implies that interband charge fluctuations arising from the quasi-1D

α, β FS sheets (xz,yz orbital character) are the “softest” (the incommensurate spin susceptibility “flattens” out to sizably lower values at low T), while the charge fluctuations in the xy-band closely track them, strongly suggesting a novel possibility for the SC mechanism, were these to be implicated in the SC pair glue. It is crucial to note that clear orbital “selectivity” reflected in our results is a consequence of the dynamical interplay between (DFT) structure (in particular, the crystal field splitting between the xz,yz and xy orbitals in the D_{4h} structure), sizable multi-orbital correlations and spin-orbital entanglement due to SOC enhanced by correlations. Thus, our analysis bares a new, hitherto unappreciated factor: the “normal” state above T_c maybe close to being electronically “soft” in the inter-orbital charge channel. A wide range of normal state responses we describe above lends strong credence to the feasibility of this conclusion.

We now qualitatively detail how these findings have novel implications for mechanism(s) for USC in Sr_2RuO_4 . The nearly soft interband charge fluctuation modes found above must overwhelm the incommensurate spin fluctuations at low T (just above T_c), raising the novel, hitherto neglected possibility that these might be primary sources for the “pair glue” leading to USC. If this be the case, our results provide support to mechanism(s)^{25–27}. Further, strong SOC also implies that these multi-orbital charge fluctuations are also intrinsically entangled⁶ with mixed spin singlet-triplet magnetic fluctuations. While Raghu *et al.* claim that USC primarily arises from the quasi-1D xz,yz bands, and that the interband proximity effect induces a secondary SC gap in the xy band²⁸, Simon *et al.* and Thomale *et al* claim, within a weak-coupling RG procedure, that all three d -bands are implicated in SC. However, our results, along with earlier local density approximation (LDA)+DMFT ones^{7,9} show that Sr_2RuO_4 is more aptly characterized as a sizably-to-strongly correlated system. The RG procedures hitherto used for study of pair symmetry are valid in the weak coupling ($U \ll W$) limit, but would be inadequate when $U \simeq W$, as appropriate here. Strictly speaking, it is possible that the weak coupling calculations identify the correct pair-symmetry if one could invoke analytic continuity from weak to the intermediate-coupling state: this maybe possible for Sr_2RuO_4 , since the low- T state immediately above T_c is a correlated FL, which is analytically continuable in the Landau sense from a weakly correlated metal. Such a study, however, remains to be done, especially within first-principles correlated approaches, and is out of scope of our present work.

The emergent low-energy picture from our normal-state results is the following: already at high T , the Hund coupling results in $S = 1$ on each Ru site, which also controls the very low $T_{FL} \simeq 23$ K via a combination of Hund metal physics¹⁰ and a dimensional crossover (see above). At high T , both the SOC as well as the (small $t_{\perp} 0.1t_{a\sigma, b\sigma'}$) interlayer hopping are irrelevant, and one can view the system in terms of an orbitally degenerate quasi-1D (xz-xyz) system coupled to a wider 2D xy-band

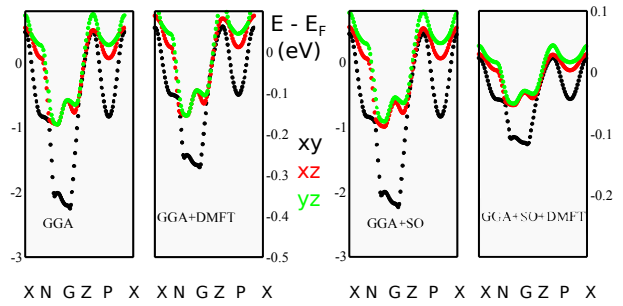


FIG. 4. DFT(GGA)+SOC results for the multi-orbital band structure of Sr_2RuO_4 . Inclusion of multi-orbital correlations leads to a sizable reduction in coherent spectral weight, which is transferred to the incoherent part of the spectral functions (not shown). From analysis of the corresponding self-energies at 30 K, we estimate effective mass enhancements of $O(3-4)$ times the band masses for the three t_{2g} orbitals, also in fair accord with dHvA estimates.

via two-body Coulomb interactions in the t_{2g} -sector. At low $T < T_{FL}$, both (especially t_{\perp}) become relevant, inducing both, spin-orbital entanglement and a dimensional crossover (see SI (ii)), resulting in an anisotropic quasi-3D correlated FL. Importantly, since sizable local interactions and SOC have already drastically renormalized the quasi-coherent part of the bare GGA band structure as shown in Fig. 4, it now follows that the “effective interactions” which finally cause cooper pairing should involve heavily renormalized, instead of bare interactions. Leaving the detailed microscopics for future, we restrict ourselves to qualitative but symmetry-based reasoning. With the assumption, bolstered by the maximally enhanced interband charge susceptibilities in the xz, yz sector in the normal-state DFT+DMFT calculation, that SC primarily arises from the quasi-1D xz-xyz bands, and noticing that only these orbitals have non-negligible overlap with out-of-plane t_{2g} orbitals in the BCT structure, we are led to a picture similar to that proposed by Hasegawa *et al.*²⁹. In the BCT structure, restricting ourselves to symmetry arguments alone leads one to a two-fold degenerate, multi-band spin-triplet and odd-parity pair state of the form

$$\Delta(k) = \mathbf{z}\Delta_0(\sin\frac{k_x a_0}{2}\cos\frac{k_y a_0}{2} + i\cos\frac{k_x a_0}{2}\sin\frac{k_y a_0}{2}).(\cos\frac{k_z c_0}{2} + a_1) \quad (3)$$

which reduces to the form $\Delta(k) = \mathbf{z}\Delta_0(k_x + ik_y)(\cos(k_z c_0) + a_1)$ for small k_x, k_y , where the a_1 component can exist on symmetry grounds in Sr_2RuO_4 ²⁹ (indeed, it results from the interband proximity-induced $(k_x + ik_y)$ gap on the xy -band). The form factor $\cos(k_z c)$ immediately leads to horizontal line nodes at $k_z = \pi/2c \pm \delta k_0$ as long as $|a_1| < 1$, as required from various data. The crucial point we wish to make is that this choice naturally results from an effective interaction which primarily couples the xz-xyz band states in the

BCT structure: the nearly soft interband charge fluctuations can also readily lead to pairing. This supports the mechanism of Raghu *et al.* The interband proximity effect will naturally induce a secondary gap of the form $\Delta_{xy}(k) \simeq \mathbf{z}(k_x + ik_y)$ on the 2D xy -band³. However, our results show that the charge susceptibility in the xy -band is also comparably enhanced, and this suggests a truly multiband modelling of the SC instability in Sr_2RuO_4 involving cooper pairs with multiband and mixed-spin character²⁶ is necessary. Whether such microscopics lead to a gap function consistent with that above remains to be seen. However, it is interesting to notice that $\Delta(k)$ arrived at from symmetry considerations above describes a two-fold degenerate state with spin-triplet character. The response to uniaxial strain discovered by Hicks *et al.*³⁰ can then be naturally understood: uniaxial strain will lift this two-fold degeneracy, stabilizing either $p_x(p_y)$ symmetries for tensile(compressive) strain (this argument cannot rationalize the enhancement of T_c under uniaxial strain, which requires full microscopics). In fact, strain must also lead to further anisotropies in the normal state responses, since LDA calculations under strain already show a Pomeranchuk-like anisotropy for the xy -(γ)-FS sheet under uniaxial strain. It would be interesting to probe this aspect in more detail in future. Moreover, while USC following from quasi-1D xz - yz bands is not of the topological type, the proximity effect restores this aspect²⁵. But given the relative weakness of the proximity coupling, one expects that the edge currents using SQUID imaging studies³¹ will have magnitudes much smaller than expected, precisely as apparently seen. Thus, a natural choice for an USC arising first in the quasi-1D bands seems to be qualitatively consistent with constraints mandated by a wide range of data. However, within the truly multiband view, Scaffidi *et al.*²⁶ posit an alternative explanation (high Chern number) for the much smaller edge currents in SQUID data, so the issue is unresolved and mandates more study. In common with most other proposals, this idea still does not fully address (i) the fact that the true situation is probably somewhere in between the proposals of Rice *et al.*³ and Raghu *et al.*, and involves all three d -bands (see, however²⁶), and (ii) more importantly, the requirement imposed by spin-orbital entanglement, namely, that the pair symmetry cannot be classified either as spin singlet or triplet when SOC is strong (the renormalized SOC is in fact larger than the renormalized crystal-field splitting in LDA+DMFT studies⁷. In fact, very recent spectroscopic evidence⁶ strongly suggests a complicated \mathbf{k} -dependent

spin-orbital entanglement. More evidence obtains from very recent strain data³², where increase of T_c under uniaxial strain is suggested to lead to a transition between two USC states having odd- and even parity: within a scenario of a pair function with an admixture of spin singlet and triplet (due to SO-entanglement), it could be that the relative weight of the singlet-triplet admixture is modified in favor of an even-parity state under strain. These requirements demand a generalization of the argument above to allow all three d -bands, and a \mathbf{k} -dependent admixture of spin singlet and triplet components into the full USC gap function, and is out of scope of this work.

CONCLUSION

To conclude, we have revisited the important issue of detailed characterization of the “normal” state in Sr_2RuO_4 using state-of-the-art first-principles correlation (GGA+SOC+DMFT(CTQMC)) approach. Armed with excellent semiquantitative accord with a wide range of normal state transport and magnetic fluctuation data, we propose that a hitherto unnoticed aspect related to dominant interband charge fluctuations from the xy , xz , yz bands potentially emerges as a new “pair glue” for USC in Sr_2RuO_4 . Assuming that these charge fluctuations are the major contributors to the pair glue, we use symmetry arguments to argue that USC with a required pair symmetry primarily arises on the α , β -FS sheets, and induces it on the quasi-2D xy -band via an interband proximity effect. However, in view of the comparable charge susceptibility from the xy -band, its contribution will also be comparable to that of the xz , yz bands in reality, necessitating a full three-band scenario in an (orbital-dependent) intermediate-to-strong coupling framework. Our study establishes a concrete link between normal state responses and the USC instability, and provides evidence that nearly soft interband charge fluctuations in the Hund metal, involving all Ru d bands potentially play an important role in fomenting USC in this system.

ACKNOWLEDGEMENTS

SA would like to acknowledge UGC (India) for a research fellowship. The authors acknowledge FIST programme of DST (India) for computational facility at the Physics Department of IIT Kharagpur.

* acharya.swagata@phy.iitkgp.ernet.in

† mslaad@imsc.res.in

‡ arghya@phy.iitkgp.ernet.in

¹ A. P. Mackenzie and Y. Maeno, *Reviews of Modern Physics* **75**, 657 (2003).

² D. A. Ivanov, *Physical Review Letters* **86**, 268 (2001).

³ M. Zhitomirsky and T. Rice, *Physical Review Letters* **87**, 057001 (2001).

⁴ C. Bergemann and A. Mackenzie and S. Julian and D. Forsythe and E. Ohmichi, *Advances in Physics* **52**, 639 (2003).

⁵ Haverkort, M. W., Elfimov, I. S., Tjeng, L. H., Sawatzky, G. A. & Damascelli, A. Strong spin-orbit coupling effects on the fermi surface of sr_2ruo_4 and sr_2rho_4 . *Phys. Rev. Lett.* **101**, 026406 (2008).

⁶ C. Veenstra *et al.*, Physical review letters **112**, 127002 (2014).

⁷ G. Zhang and E. Gorelov and E. Sarvestani and E. Pavarini, Physical review letters **116**, 106402 (2016).

⁸ X. Deng and K. Haule and G. Kotliar, arXiv preprint arXiv:1504.00292 (2015).

⁹ J. Mravlje and M. Aichhorn and T. Miyake and K. Haule and G. Kotliar and A. Georges, Physical Review Letters **106**, 096401 (2011).

¹⁰ J. Mravlje and A. Georges, arXiv preprint arXiv:1504.03860 (2015).

¹¹ Bauer, B. *et al.* The alps project release 2.0: open source software for strongly correlated systems. *Journal of Statistical Mechanics: Theory and Experiment* **2011**, P05001 (2011).

¹² P. Blaha and K. Schwarz and G. Madsen and D. Kvasnicka and J. Luitz, An augmented plane wave+ local orbitals program for calculating crystal properties (2001).

¹³ A. A. Mostofi and J. R. Yates and Y.-S. Lee and I. Souza and D. Vanderbilt and N. Marzari, Computer physics communications **178**, 685 (2008).

¹⁴ J. Kuneš and R. Arita and P. Wissgott and A. Toschi and H. Ikeda and K. Held, Computer Physics Communications **181**, 1888 (2010).

¹⁵ Q. Si, S. Rabello, K. Ingersent and J-L Smith, Nature **413**, 804 (2001).

¹⁶ P. W. Anderson, Nature Physics **2**, 626 (2006).

¹⁷ A. Georges and T. Giamarchi and N. Sandler, Physical Review B **61**, 16393 (2000).

¹⁸ T. Katsufuji and M. Kasai and Y. Tokura, Physical review letters **76**, 126 (1996).

¹⁹ M. Braden and Y. Sidis and P. Bourges and P. Pfeuty and J. Kulda and Z. Mao and Y. Maeno, Physical Review B **66**, 064522 (2002).

²⁰ M. Braden and O. Friedt and Y. Sidis and P. Bourges and M. Minakata and Y. Maeno, Physical review letters **88**, 197002 (2002).

²¹ R. Werner and V. Emery, Physical Review B **67**, 014504 (2003).

²² K. Ishida and H. Mukuda and Y. Kitaoka and Z. Mao and H. Fukazawa and Y. Maeno, Physical Review B **63**, 060507 (2001).

²³ A. Damascelli *et al.*, Physical review letters **85**, 5194 (2000).

²⁴ A. Liebsch and A. Lichtenstein, Physical review letters **84**, 1591 (2000).

²⁵ S. Raghu and A. Kapitulnik and S. Kivelson, Physical review letters **105**, 136401 (2010).

²⁶ T. Scaffidi and J. C. Romers and S. H. Simon, Physical Review B **89**, 220510 (2014).

²⁷ Q. H. Wang and C. Platt and Y. Yang and C. Honerkamp and F. C. Zhang and W. Hanke and T. M. Rice and R. Thomale, Europhysics Letters **104**, 1, 17013 (2013).

²⁸ D. Agterberg and T. Rice and M. Sigrist, Physical review letters **78**, 3374 (1997), G. Baskaran, *Physica B: Condensed Matter*, **223-224**, 490-495 (1996).

²⁹ Y. Hasegawa and K. Machida and M.-a. Ozaki, Journal of the Physical Society of Japan **69**, 336 (2000).

³⁰ C. W. Hicks and D. O. Brodsky and E. A. Yelland and A. S. Gibbs and J. A. N. Bruin and M. E. Barber and S. D. Edkins and K. Nishimura and S. Yonezawa and Y. Maeno and A. P. Mackenzie, *Science* **344**, 283 (2014), <http://science.sciencemag.org/content/344/6181/283.full.pdf>.

³¹ J. Kirtley *et al.*, Physical Review B **85**, 224518 (2012).

³² A. Steppke *et al.*, arXiv preprint arXiv:1604.06669 (2016).